ChemComm

RSC Publishing

COMMUNICATION

View Article Online
View Journal

A phenyl-capped aniline tetramer for Z907/*tert*-butylpyridine-based dye-sensitized solar cells and molecular modelling of the device†

Cite this: DOI: 10.1039/c2cc38625a

Received 1st December 2012,
Accepted 21st December 2012

DOI: 10.1039/c2cc38625a

www.rsc.org/chemcomm

Kazuhiro Manseki,*[ab] Youhai Yu[ac] and Shozo Yanagida*[ad]

Z907-sensitized solar cells incorporating a phenyl-capped aniline tetramer (EPAT) as a substitute of the iodine/iodide redox couple in the electrolytes produce an enhanced open-circuit voltage and short circuit photocurrent density when *tert*-butylpyridine (TBP) is added to the electrolyte.

Dye-sensitized solar cells (DSCs) have been regarded as a promising cost-effective technology for roof-top solar panels and various indoor applications.[1] Most high-performance titanium dioxide (TiO_2) DSCs reported so far significantly rely on low-cost iodine electrolytes. This is because iodine/iodide redox couples can infiltrate deep inside the nano-sized pores of the titania layers and provide a favorable source of conductance of the polyiodide species, resulting in a respectable photovoltaic performance.[2] On the other hand, iodine redox shuttles have the following disadvantages in terms of cell performance and robustness: (i) absorption of visible light ($\lambda = \sim 430$ nm) leading to a photocurrent loss by the DSCs, (ii) corroding grid metals such as silver and platinum on cathodes due to the sublimation and strong oxidizing nature of iodine, and (iii) a significant photocurrent loss, particularly in highly viscous electrolyte-based DSCs. As a cost-effective alternative to conventional iodine systems, Kanatzidis *et al.* very recently reported high-efficiency iodine-free DSCs with a novel solution-processable inorganic hole-transport material.[3] In view of this finding, hole transport materials that possess a high mobility and mediate the recovery of oxidized dye molecules at the dye interface could allow further development of durable and efficient DSCs. As iodine-free DSCs could be beneficial for practical applications, we believe that one of the most promising routes is to make use of the advantage of new non-corrosive charge transport material systems for the development of DSCs.

In our earlier work, electrically conducting polymers, such as polyaniline, poly(3,4-ethylenedioxythiophene) (PEDOT) and poly-3-hexylthiophene (P3HT), have been applied to mesoscopic TiO_2-based DSCs.[4,5] Such large molecular polymers often cause a difficulty in infiltrating into the interwined nanopores of the photoelectrodes. For solid-state DSCs, a major issue has been placed on interface engineering of the TiO_2/dyes/hole transport materials. We and other groups have demonstrated the remarkable improvement of DSC performance by introducing *in situ* photo-electropolymerization methods for filling conducting polymers into the nanopores of dye-absorbed TiO_2 electrodes.[6]

This communication describes a phenyl-capped aniline tetramer that works as a novel organic conductive redox mediator in a Z907-based DSC (Z907: *cis*-bis(isothiocyanato)(2,2′-bipyridyl-4,4′-dicarboxylato)(2,2′-bi-pyridyl-4,4′-di-nonyl ruthenium(II)), and the results are rationalized by a computational molecular modelling using the density functional theory (DFT). As shown in Fig. 1, the low-molecular phenyl-capped polyaniline tetramer can be expressed by four oligoaniline structures, *i.e.*, fully-reduced leucoemeraldine-type (LPAT), half-oxidized emeraldine-type (symmetrical and unsymmetrical) (EPAT), and fully-oxidized pernigraniline-type

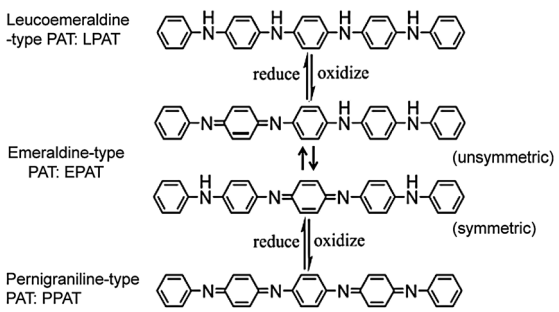

Fig. 1 Chemical structure of phenyl-capped aniline tetramers.

[a] *Center for Advanced Science and Innovation, Osaka University, Yamadaoka 1-1, Suita, Osaka, Japan*
[b] *Graduate School of Engineering, Environmental and Renewable Energy System (ERES) Division, Gifu University, 1-1, Yanagido, Gifu 501-1193, Japan. E-mail: kmanseki@gifu-u.ac.jp*
[c] *Centre d Investigacio en Nanociencia i Nanotecnologia (CIN2, CSIC), Campus UAB, Edifici ETSE 2nd Floor, Bellaterra, Barcelona, E-08193, Spain*
[d] *ISIR, Osaka University, 2-1, Mihoga-oka, Ibaraki, Osaka, 567-0047, Japan. E-mail: yanagida@mls.eng.osaka-u.ac.jp*

† Electronic supplementary information (ESI) available: Experimental details including DSC assembly and results of other DFT calculations. See DOI: 10.1039/c2cc38625a

(PPAT), which have structures similar to polyaniline derivatives often utilized for organic electronic devices.[7,8] A reversible redox property was clearly observed for the 1 M H_2SO_4 solution of EPAT (see Fig. S1, ESI†) and the onset potential of the first oxidation state appeared at 650 mV. The highest occupied molecular orbital (HOMO) was estimated to be at −5.05 eV, which is close to that of the iodine/iodide redox potential (−5 eV). We anticipated that EPAT works as a redox mediator in the DSCs.

A violet powder of EPAT was prepared by a literature method.[9] This gave a UV/Vis absorption spectrum in DMF (Fig. S2a, ESI†). The computational UV/Vis spectra of four aniline structures revealed that they are well consistent with tectrum of the as-prepared EPAT matches that of the symmetrical EPAT (Fig. S2 and S3, ESI†). The large absorption intensity at a shorter wavelength could be rationalized as being due to the contribution of the unsymmetrical EPAT. In fact, the analysis of the thermodynamic energy data of the DFT modelling indicated that the formation of the symmetrical EPAT is slightly favored compared to the unsymmetrical species by 0.71 kcal mol^{-1} (see Table S1, ESI†).

EPAT-based DSCs were found to work when Z-907 is employed as a photosensitizing dye and assembled with the electrolyte composed of EPAT, *tert*-butylpyridine (TBP) and valeronitrile. Fig. 2 shows the best *I–V* data of the DSCs. The optimized DSC gave a short-circuit photocurrent density of 8.41 mA cm^{-2}, an open circuit voltage of 584 mV, and a fill factor of 0.575, corresponding to an overall conversion efficiency of 2.82%. We also tested the cell performance by using the benchmark Ru dye of *cis*-bis(isothiocyanato) bis-(2,2′-bipyridyl-4,4′-dicarboxylate) ruthenium(II) bis-tetra-*n*-butyl-ammonium (N719). N719 exhibited a very low cell performance ($\eta < 0.1\%$), even though the redox potential of the HOMO level of Z907 is slightly positive than the value of N719 [0.80 V *vs.* a saturated calomel reference electrode (SCE)].[10]

We found that the cell performance of our EPAT-based DSCs is significantly enhanced by the addition of TBP to the electrolyte (Fig. 3). The addition of TBP increased the open-circuit voltage (V_{oc}) by about 100 mV as already demonstrated by the iodine/iodide-based electrolyte systems.[11] The effect of TBP on the V_{oc} can be explained as due to the conduction band shift of TiO_2 by basic TBP in the vicinity of the TiO_2 surface.[12] In addition, the short-circuit photocurrent (J_{sc}) also increased with the addition of TBP by a factor of 3 together with the increase in the V_{oc}. This result presents a sharp contrast to those that have been reported for iodine/iodide-based DSCs.

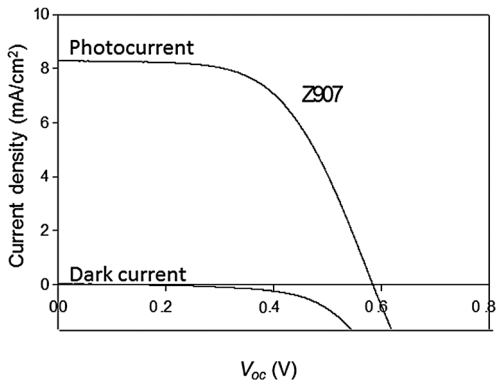

Fig. 2 *I–V* curves of the best performing cell with Z907 dye irradiated under simulated one sunlight conditions. EPAT was used as the redox mediator in the DSC. The performance was optimized using 8 μm titania nanocrystalline films (Table 1).

Table 1 Photovoltaic performance of DSCs obtained from *I–V* data

Dye molecule	TiO_2 thickness (μm)	V_{oc} (mA cm^{-2})	J_{sc} (mA cm^{-2})	FF	η (%)
Z907	4	583 ± 10	6.15 ± 0.20	0.61 ± 0.01	2.18 ± 0.01
Z907	8	583 ± 13	8.29 ± 0.30	0.58 ± 0.01	2.80 ± 0.10
Z907	12	542 ± 17	6.28 ± 0.30	0.57 ± 0.01	1.93 ± 0.09
N719	8	144 ± 8.0	0.96 ± 0.04	0.26 ± 0.02	0.04 ± 0.01

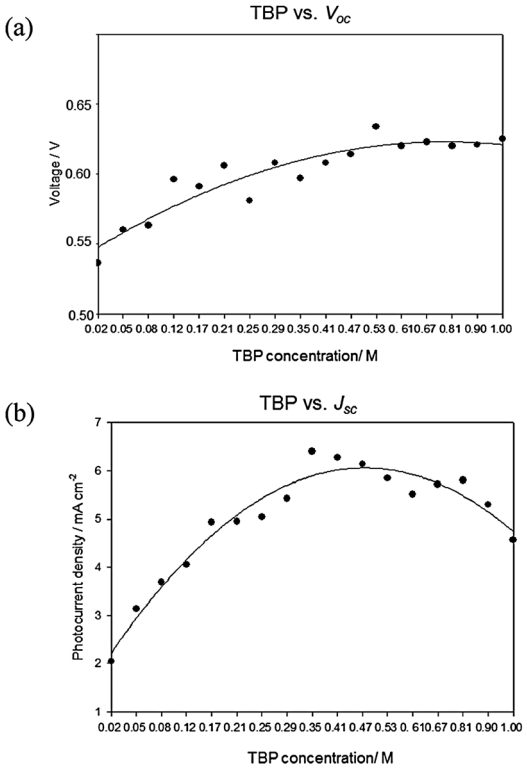

Fig. 3 Effects of TBP addition on the cell performance of V_{oc} and J_{sc}. The data (a, b) were plotted from the *I–V* measurements of DSCs containing TBP as an additive in the electrolyte.

Density functional theory (DFT)-based molecular modelling coupled with molecular mechanics calculations makes it possible to evaluate the equilibrium geometry (bond lengths, bond angles and dipole moments) and energy structures of the highest occupied molecular orbital (HOMO) and the lowest unoccupied molecular orbital (LUMO) that are associated with the non-bonding van der Waals interaction, *i.e.*, π–π stacking, hydrogen–π stacking, and hydrogen bonding.[2] The molecular modelling of the interaction between the EPAT and TBP was successfully performed using DFT at the B3LYP/6-31G(d) level with Spartan 10. All energy structures and dipole moment data are summarized in Table S1 (ESI†) together with those of the symmetrical and unsymmetrical EPAT, TBP, Z907 and N3 as a substitute of N719. It is worth noting that symmetrical EPAT is thermodynamically more stable than the unsymmetrical one, and that the symmetrical EPAT favors

the interaction with TBP either *via* hydrogen bonding or *via* hydrogen–π stacking (see Fig. S4, ESI†).

The HOMO energy level of EPAT (symmetrical) was determined to be −4.72 eV, whereas Z907 showed the more negative potential of −4.52 eV. On the other hand, EPAT associating with TBP (TBP–EPAT) through hydrogen-bonding produced an energy level of −4.47 eV. In fact, the interaction of EPAT with TBP through hydrogen bonding is much more favorable than the van der Waals interaction by 5.7 kcal mol^{-1} based on the analysis of the thermodynamic energy data (see Table S1, ESI†). Conversely, the HOMO level of N3 (N719) is still more positive than that of TBP–EPAT, rationalizing the poor result for the N719-sensitized DSC. It is also noteworthy that the high dipole moment of 2.53–5.71 debye was determined as a result of the formation of a hydrogen-bonding complex of TBP–EPAT. These facts indicated that TBP allows the efficient infiltration of fluid EPAT solutions into the mesoscopic TiO_2 layers. It is thus postulated that the penetration of EPAT into the vicinity of Z907 on TiO_2 leads to the self-association of Z907 with EPAT.

In order to confirm that EPAT undergoes a self-organization through the non-bonded interaction with the alkyl chains in Z907, the interactions of EPAT with *n*-nonane, *n*-nonylbenzene, and Z907 with energetically most stable zigzag linear nonyl groups were separately simulated by DFT by taking into account energy relationship and the shape of the frontier orbitals of the respective molecules as in the case of TBP (see Fig. S5–S7, ESI†). These results indicated that the frontier orbitals, *i.e.*, the HOMO and LUMO of EPAT, interact with the respective LUMO and HOMO of each molecule, leading to the successful modelling of the nonbonding interaction of EPAT not only with *n*-nonane and *n*-nonylbenzene but also with Z907. The equilibrium geometry of the associated EPAT/*n*-nonane and EPAT/*n*-nonylbenzene gave a non-bonded interaction through the hydrogen–nitrogen bond and/or hydrogen–π-stacking. They are comparable to the so-called van der Waals distance (∼3.6 Å). However, the energy levels of the HOMO and the LUMO are located only on the EPAT molecule with the similar energy level of sole EPAT. On the other hand, the EPAT/Z907 simulation gave the equilibrium geometry in which the HOMO is located on Z907 and the LUMO on EPAT (Fig. S7b, ESI†). These facts suggested that the interaction is stronger than the EPAT–TBP interaction. In addition, the electrostatic potential map indicated that the nearest distance between the sulfur of Z907 and hydrogen on the nitrogen of EPAT is 2.511 Å (Fig. 4). Therefore, such a self-organized association of EPAT with Z907 must operate concurrently on the Z907-adsorbed TiO_2, resulting in the increase in both J_{sc} and V_{oc} for the present Z907/TBP-based DSC.

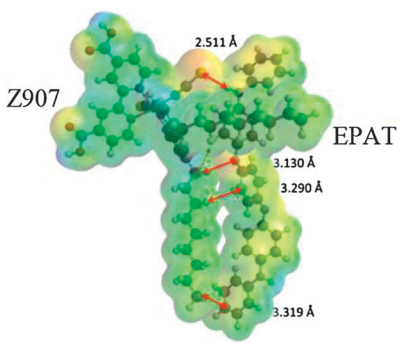

Fig. 4 Electrostatic potential map and specific non-bond distance in the associated molecule of Z907/EPAT.

We demonstrated that a new iodine-free electrolyte containing a phenyl-capped aniline tetramer EPAT produces the maximum overall conversion efficiency (η) of 2.82% for the Z907 sensitizing DSC in the presence of TBP in the electrolytes. The TBP positive effects were clarified not only by a V_{oc} increase as often pointed out in the iodine/iodide-based DSC, but also by a remarkable J_{sc} increase. DFT-based molecular modelling suggested the importance of interactions *via* HOMO–LUMO non-bonding interaction of EPAT with both TBP and Z907.[2] Although the efficiency is still low compared to those of the iodine/iodide based DSC, we envisage that the phenyl-capped aniline tetramer derivatives will be a promising electron-transfer mediator for the iodine-free DSC. In addition, the long-term durability would benefit from such oligoaniline-based DSCs that could avoid the corrosion of grid metals. The molecular orbital design for the successful optimization of unidirectional electron flow in the TiO_2/dyes/oligoaniline-liquid device will shed light on the advanced development of low-cost, robust and highly efficient DSCs.

One of the authors (K.M.) acknowledges the support from The Koshiyama Research Grant and The Advancing Researcher Support Program (Gifu University, Faculty of Engineering).

Notes and references

1 Recent examples: A. Hagfeldt, G. Boschloo, L. Sun, L. Kloo and H. Petterson, *Chem. Rev.*, 2010, **110**, 6595; B. E. Hardin, H. J. Snaith and M. D. McGehee, *Nat. Photonics*, 2012, **6**, 162; Q. Zhang and G. Cao, *Nano Today*, 2011, **6**, 91.
2 F. C. Küpper, M. C. Feiters, B. Olofsson, T. Kaiho, S. Yanagida, M. B. Zimmermann and L. J. Carpenter, *Angew. Chem., Int. Ed.*, 2011, **50**, 11598.
3 I. Chung, B. Lee, J. He, R. P. H. Chang and M. G. Kanatzidis, *Nature*, 2012, **485**, 486.
4 J. Xia and S. Yanagida, *Sol. Energy*, 2011, **85**, 3143.
5 S. Yanagida, Y. Yu and K. Manseki, *Acc. Chem. Res.*, 2009, **42**, 1827.
6 K. Manseki, W. Jarernboon, Y. Yu, K.-J. Jiang, K. Suzuki, N. Masaki, Y. Kim, J. Xia and S. Yanagida, *Chem. Commun.*, 2011, **47**, 3120; A. Mozer, D. Panda, S. Gambhir, B. Winther-Jensen and G. Wallace, *J. Am. Chem. Soc.*, 2010, **132**, 9543; X. Liu, W. Zhang, S. Uchida, L. Cai, B. Liu and S. Ramakrishna, *Adv. Mater.*, 2010, **22**, E150; X. Liu, Y. Cheng, L. Wang and B. Liu, *Phys. Chem. Chem. Phys.*, 2012, **14**, 7098.
7 A.-G. MacDiarmid, *Angew. Chem., Int. Ed.*, 2001, **40**, 2581.
8 D.-M. Sarno, S.-K. Manohar and A.-G. MacDiarmid, *Synth. Met.*, 2005, **148**, 237.
9 J. Gao, K. Li, W. Zhang, C. Wang, Z. Wu, Y. Ji, Y. Zhou, M. Shibata and R. Yosomiya, *Macromol. Rapid Commun.*, 1999, **20**, 560.
10 S. M. Zakeeruddin, M. K. Nazeeruddin, R. Humphry-Baker, P. Péchy, P. Quagliotto, C. Barolo, G. Viscardi and M. Grätzel, *Langmuir*, 2002, **18**, 952.
11 S. Zhang, X. Yang, K. Zhang, H. Chen, M. Yanagida and L. Han, *Phys. Chem. Chem. Phys.*, 2011, **13**, 19310; G. Boschloo, L. Haggman and A. Hagfeldt, *J. Phys. Chem. B*, 2006, **110**, 13144; S. Zhang, M. Yanagida, X. Yang and L. Han, *Appl. Phys. Express*, 2011, **4**, 042301; K. Zhang, S. Zhang, K. Sodeyama, X. Yang, H. Chen, M. Yanagida, Y. Tateyama and L. Han, *Appl. Phys. Express*, 2012, **5**, 042303.
12 For example: M. K. Nazeeruddin, A. Kay, I. Rodicio, R. Humphry-Baker, E. Muller, P. Liska, N. Vlachopoulos and M. Grätzel, *J. Am. Chem. Soc.*, 1993, **115**, 6382; S. Nakade, T. Kanzaki, W. Kubo, T. Kitamura, Y. Wada and S. Yanagida, *J. Phys. Chem. B*, 2005, **109**, 3480.